

Review

# Rational Design of Nanozymes Enables Advanced Biochemical Sensing

Jinjin Liu <sup>1</sup> and Xiangheng Niu <sup>1,2,\*</sup> <sup>1</sup> School of Public Health, Hengyang Medical School, University of South China, Hengyang 421001, China<sup>2</sup> Institute of Green Chemistry and Chemical Technology, School of Chemistry and Chemical Engineering, Jiangsu University, Zhenjiang 212013, China

\* Correspondence: niuxiangheng@usc.edu.cn

**Abstract:** In comparison with bioenzymes, nanozymes exhibit excellent robustness against extreme conditions, a low production cost, and easy-to-adjust properties, as well as potential versatility. These superiorities have attracted abundant interest in the last 15 years, to develop various nanozymes for applications including analytical sensing, environmental engineering, and biomedicine. In particular, for analytical sensing, a lot of nanozyme-involved principles and methods have been explored and applied to clinical diagnosis, environmental monitoring, food safety detection, and forensic analysis. Moreover, rational exploitation and use of nanozyme materials promote the performance of analytical methods. To highlight the latest progress in this attractive field, recent design concepts of nanozymes for advanced biochemical sensing are summarized. The development of single-atom nanozymes, self-cascade nanozymes, structurally biomimetic nanozymes, molecularly imprinted nanozymes, nanozymes breaking the pH limit, and multifunctional nanozymes is discussed in detail, to enhance detection sensitivity and selectivity, as well as expand application scenarios. Finally, some challenges and trends related to nanozyme-based sensors are reported, to satisfy the increasing needs of biochemical analysis with nanozymes.

**Keywords:** nanozyme; rational design; biochemical detection; sensitivity; selectivity; application scenario



**Citation:** Liu, J.; Niu, X. Rational Design of Nanozymes Enables Advanced Biochemical Sensing. *Chemosensors* **2022**, *10*, 386. <https://doi.org/10.3390/chemosensors10100386>

Academic Editor: Barbara Palys

Received: 8 September 2022

Accepted: 21 September 2022

Published: 23 September 2022

**Publisher's Note:** MDPI stays neutral with regard to jurisdictional claims in published maps and institutional affiliations.



**Copyright:** © 2022 by the authors. Licensee MDPI, Basel, Switzerland. This article is an open access article distributed under the terms and conditions of the Creative Commons Attribution (CC BY) license (<https://creativecommons.org/licenses/by/4.0/>).

## 1. Introduction

Nanozymes are defined as a class of nanoscale materials that are able to exhibit enzyme-like catalytic behaviors, kinetics, and mechanisms [1–3]. As an emerging member of artificial enzymes, nanozymes have experienced a period of explosive development in the past 15 years [4]. In contrast to natural bioenzymes, they show several attractive characteristics and benefits, including an excellent stability, even under harsh conditions, easy scale production, low cost, and easy-to-regulate catalytic performance. Compared to the previously developed organic artificial enzymes (cyclodextrins, porphyrins, supermolecules, et al.), the unique feature of an inorganic nanostructures can endow nanozymes with potential versatility [5]. These advantages are drawing more and more interest, to explore nanozymes for various applications, such as analytical sensing, environmental engineering, and biomedicine. In the analytical sensing field, the signal amplification offered by catalytic reactions makes nanozymes promising enzyme alternatives for developing a number of analytical principles and methods [6]. Commonly, nanozymes are used as catalysts to trigger a series of chromogenic, fluorescence, or chemiluminescence reactions, thus providing optical signals for the qualitative and quantitative determination of targets. They can replace horseradish peroxidase (HRP) or alkaline phosphatase (ALP) as catalytic labels to fabricate immunoassays [7]. In addition, the conjugation of nanozymes with other sensing elements (DNA chains, aptamers, bioenzymes, et al.) enables the development of multifarious sensors [8]. In addition, interactions between certain species and nanozyme surfaces make it possible to realize the detection of the former [9].

These principles and methods have given nanozymes intensive use in clinical diagnosis, biochemical measurement, environmental monitoring, food safety analysis, and forensic detection [10–12].

Undoubtedly, the introduction of nanozymes opens a new path to obtaining high-performance sensing. A variety of chemosensors and biosensors have been fabricated based on nanozyme catalysis in the last decade [13]. Even so, in this field some issues remain that seriously hinder the further development of nanozyme-based biochemical sensing and need to be addressed. For instance, a large number of the nanozymes explored currently lack catalytic specificity, and achieving selective detection with nanozymes becomes a crucial problem [14]. The catalytic activity of nanozymes is still far lower than that of corresponding natural enzymes, and how to utilize nanozymes for a highly sensitive analysis, particularly for ultratrace targets, is challenging. Furthermore, expanding the applicability of nanozyme-based analytical methods in complex scenarios is always desirable.

To solve the above issues, the rational design of nanozymes, based on deeply understanding their structures and mechanisms, to gain the desired catalytic features is necessary [15]. To date, several emerging material strategies have been demonstrated as successful for significantly accelerating the development of chemosensors and biosensors. To highlight the progress in this interesting field, here we aimed at summarizing recent nanozyme concepts for promoting biochemical sensing (Figure 1). The rational design of single-atom nanozymes with extraordinary activity, as well as self-cascade nanozymes with multiple signal amplifications, was reviewed, to enhance detection sensitivity. For selectivity improvement, structurally biomimetic nanozymes and molecularly imprinted nanozymes are introduced in detail. To expand the application scenarios, the development of nanozymes breaking the pH limit, as well as multifunctional nanozymes with luminescent properties, is discussed. At the end of this review, to attract more efforts toward meeting increasing analytical requirements, some challenges and trends in the designing and development of nanozymes for advanced biochemical sensing are presented.

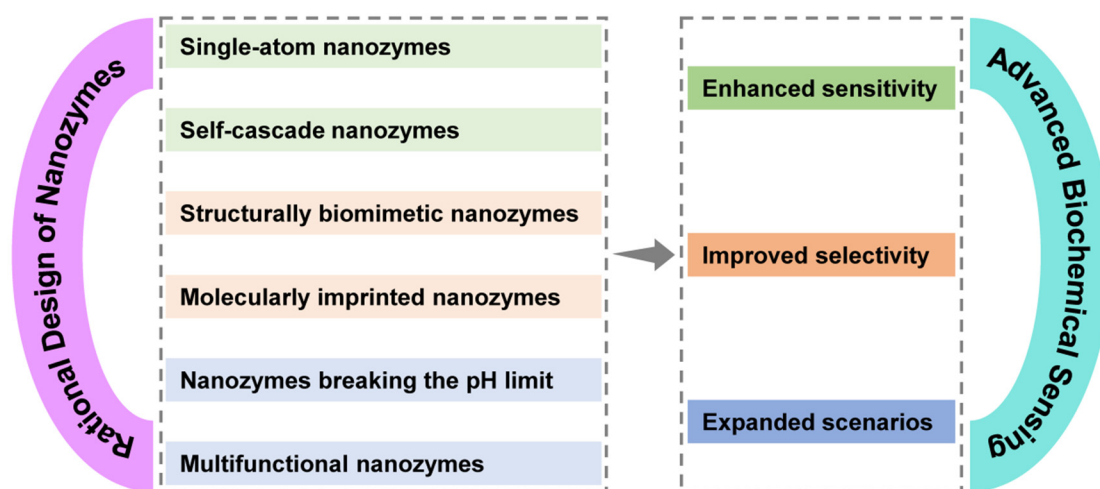


**Figure 1.** Diagram for the rational design of nanozymes, enabling advanced biochemical sensing.

## 2. Rational Design of Nanozymes for Enhancing Detection Sensitivity

Sensitivity is considered one of the most important analytical parameters for a sensor. In nanozyme-based chemosensors and biosensors, the detection sensitivity closely relies on the catalytic activity of the materials used. Although the signal amplification provided by a nanozyme catalysis is able to offer acceptable sensitivity for conventional sensing, detecting ultratrace analytes requires exploring enzyme mimics with the desired activity. However, the catalytic activity of most nanozymes developed currently is far lower than that of the corresponding bioenzymes. Designing and developing high-activity nanozymes has become a vital topic in the community. To date, several strategies, including structural

engineering [16], size regulation [17–19], surface modification [9,20], doping effect [21–23], and material compositing [24] have been explored to improve the catalytic activity of nanozymes. Given that these traditional strategies have been summarized in some other publications [25,26], we will not repeat these nanozyme activity enhancement methods here. Instead, two emerging material strategies, namely single-atom nanozymes and self-cascade nanozymes, are discussed for improving the detection sensitivity of nanozyme-involved sensors.

### 2.1. Single-Atom Nanozymes

Since the concept of single atomic catalysts (SACs) was first proposed by Qiao et al. to promote CO oxidation with a high activity [27], it has attracted intensive attention and interest from the academic community [28,29]. SACs consist of atomic active sites highly dispersed on inert carriers and are generally regarded as the limit for the design of nanoscale materials at the atomic level. When SACs are employed as enzyme mimics, namely single-atom nanozymes (SANs), some interesting features and benefits appear [30]. First, the atomic active sites of many SANs are very similar to those of metal-containing bioenzymes [31], and such a structural similarity can inspire the design of nanozymes with high activity and substrate specificity [32]. Second, SANs have well-defined geometric and electronic structures, which help the study of the catalytic processes and mechanisms of nanozymes [33,34]. Third, it is relatively easy to regulate the active site microenvironment of SANs, thus facilitating the study of the structure–activity relationship [35]. Fourth, SANs have a maximum atomic utilization efficiency and can be cycled for reuse, satisfying the green and economical principles of materials. Last but not least, although SANs belong to the heterogeneous catalysts, the high dispersion of active sites enables them to possess some characteristics of homogeneous catalysts [30]. As a result, a number of SACs have been explored as artificial enzymes for various applications in recent years [34,36–38], demonstrating that single atomization is an efficient way to gain high-activity nanozymes [39].

With the above features, SANs not only provide ideal models for studying sensing mechanisms, but also endow nanozyme-based sensors with the desired performance [40]. In this regard, several SANs with high activity have been explored and applied to analytical sensing [41–45], and some of them can even provide higher sensitivity and lower limit of detection (LOD) compared to bioenzymes [43]. Cheng et al. developed a CNT/FeNC SAN with high peroxidase-like activity for ultrasensitive biosensing [41]. They first dispersed oxidized carbon nanotubes (CNTs) in a pyrrole solution, where pyrrole could be adsorbed onto CNTs because of the  $\pi$ - $\pi$  interaction between the carbon planes of CNTs and the pyrrole molecules (Figure 2A). Then, they triggered the polymerization of pyrrole adsorbed on CNTs, to form polypyrrole (PPy), using  $(\text{NH}_4)_2\text{S}_2\text{O}_8$  as an oxidant. After that, the obtained CNT/PPy was impregnated in a mixture of  $\text{Fe}(\text{NO}_3)_3$  and NaCl to adsorb metal cations, followed by pyrolyzing the collected solid hybrid in  $\text{N}_2$  and  $\text{NH}_3$  atmospheres successively, thus obtaining CNT/FeNC SAN. The gained SAN theoretically had 100% atomic Fe– $\text{N}_x$ –C moieties, exhibiting excellent peroxidase-mimicking catalytic activity to trigger the oxidation of several chromogenic substrates in the presence of  $\text{H}_2\text{O}_2$ . With the superior SAN, they developed paper-based bioassays for  $\text{H}_2\text{O}_2$  and ascorbic acid (AA). Detection of glucose was also achieved when combining the SAN with glucose oxidase (GOx).

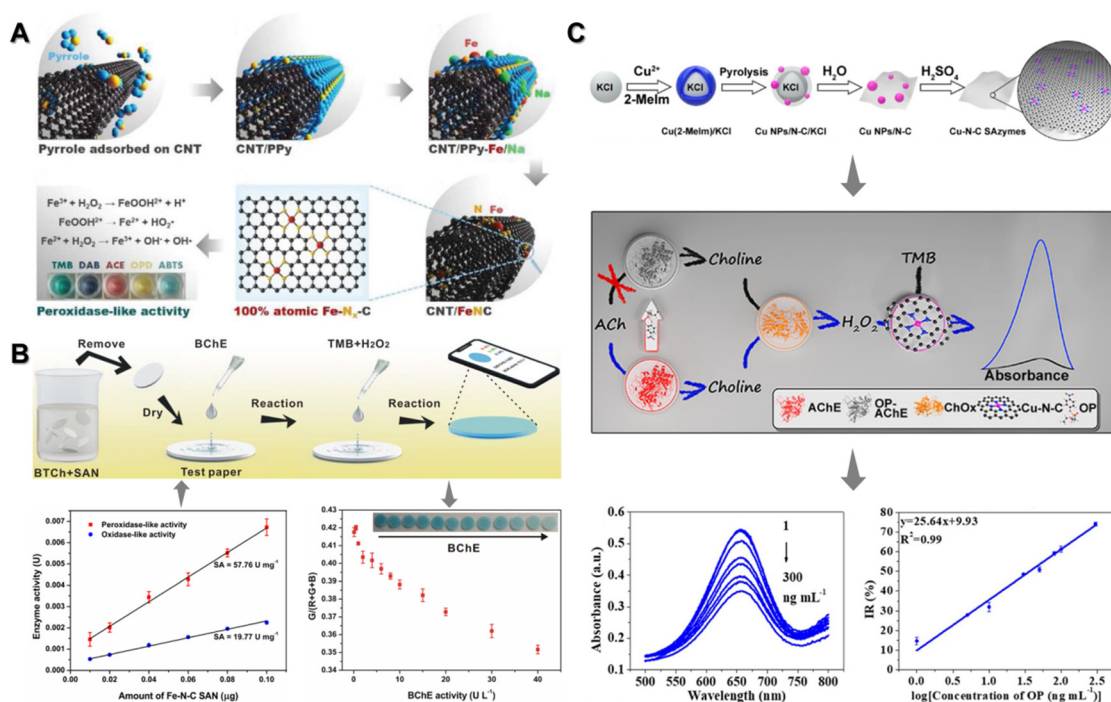


**Figure 2.** (A) Preparation of CNT/FeNC SAN with a high peroxidase-mimetic activity (reprinted with permission from Ref. [41]). (B) Fe-N-C SAN with prominent peroxidase-mimicking activity for paper-based bioassay of BChE activity (reprinted with permission from Ref. [44]). (C) Design of Cu-N-C SAN with rich Cu sites for organophosphorus sensing (reprinted with permission from Ref. [46]).

Apart from the above synthetic strategy, calcination of metal–organic frameworks (MOFs) is another widely used method to gain SANs with an outstanding catalytic activity [44,45,47]. Our group synthesized a Fe-N-C SAN with single-atom Fe-N<sub>x</sub> entities stabilized by MOFs-derived carbon, which could present peroxidase-like activity almost at the same level as natural HRP [44]. The Fe-N-C SAN was prepared by successively pyrolyzing a FeZn MOF in different atmospheres, followed by washing off large metal and metal oxide particles with acid. It was found that the obtained Fe-N-C SAN exhibited both peroxidase- and oxidase-like catalytic activities in acidic media. By employing 3,3',5,5'-tetramethylbenzidine (TMB) as a substrate, the catalytic activity of the Fe-N-C SAN was carefully evaluated according to the standard protocol [48]. Consequently, the SAN provided a specific peroxidase-like activity up to 57.76 U/mg, which was comparable to natural HRP (Figure 2B). With this exceptional activity, we further fabricated a smartphone-assisted paper-based bioassay for the monitoring of butyrylcholinesterase (BChE), a typical biomarker of organophosphorus and carbamate pesticide residues. As a result, the bioassay provided linear responses for BChE activity in the range of 2~40 U/L, with a detection limit lower than most previous methods.

In many SACs and SANs, the content of single metal atoms acting as catalytic active sites is very low (less than 1.5 wt%), seriously hindering their mass activity and advanced applications [49]. To further improve the activity of SANs and their sensing sensitivity, exploring effective methods to fabricate SANs with high metal loading is required. In this regard, Zhu's group designed a Cu-based SAN with abundant Cu sites (up to 5.1 wt%) loaded on carbon nanosheets using a salt-template strategy (Figure 2C), which exhibited excellent enzyme-like activity and enhanced biosensing performance [46]. It should be noted that the obtained Cu-N-C SAN only exhibited peroxidase-like catalytic activity, but no oxidase-like activity. This feature could effectively avoid the background brought by the oxidase-mimetic activity during biosensing. By integrating the Cu-N-C SAN with natural acetylcholinesterase (AChE) and choline oxidase (ChO), they fabricated a triple-enzyme

cascade reaction system for the colorimetric determination of acetylcholine (ACh) and organophosphorus (OP) with enhanced sensitivity.

## 2.2. Self-Cascade Nanozymes

Cascade biocatalysis commonly occurs in living organisms, to control the metabolism and signal transduction. In a cascade biocatalytic system, multiple bioenzymes are often involved in triggering two or more reactions, where each subsequent reaction begins after the previous one is completed. Given multi-enzyme-driven cascade reactions can provide superior activity and selectivity, a lot of systems have been developed as biomimetic reactors for biosensing and biomedical applications [50,51]. With increasing materials being found to exhibit multiple enzyme-like activities [52–55], instead of using several enzyme mimics to fabricate a cascade catalytic system, it is preferable to design nanozymes with self-cascade catalytic properties, where cascade reactions occur on the surface of a single nanozyme. As a result, the proximity effect of different active sites, as well as the shortened intermediate diffusion, can provide a higher catalytic efficiency [56,57]. With this attractive feature, self-cascade nanozymes have found promising use in biomedicine [58–62].

For analytical sensing, self-cascade catalytic reactions are able to offer multiple amplifications of signals (Figure 3A). Correspondingly, a higher detection sensitivity is supposed to be obtained in comparison with sensors based on single catalysis. As a common example, several Cu-based materials have been explored as self-cascade nanozymes for biosensing [63–67], where their oxidase- and peroxidase-like activities are mainly employed. We designed a Cu-based MOF material (CuBDC) that acted as a self-cascade nanozyme with cysteine oxidase- and peroxidase-mimetic catalytic activities [63]. In this material, the Cu–O clusters not only showed the capacity for catalyzing the oxidation of cysteine with the help of dissolved O<sub>2</sub> to produce cystine and H<sub>2</sub>O<sub>2</sub>, but also provided the peroxidase-mimetic ability for catalyzing the generated H<sub>2</sub>O<sub>2</sub> to produce radicals under the same conditions. Given that the terephthalic acid (TA) ligand of the MOF could be oxidized to fluorescent 2-hydroxyterephthalic acid (TAOH) by the produced radicals, the CuBDC presented a remarkable fluorescence when cysteine was fed (Figure 3B). Such a system catalyzed by the self-cascade nanozyme offered an efficient method to sensitively detect the cysteine substrate.

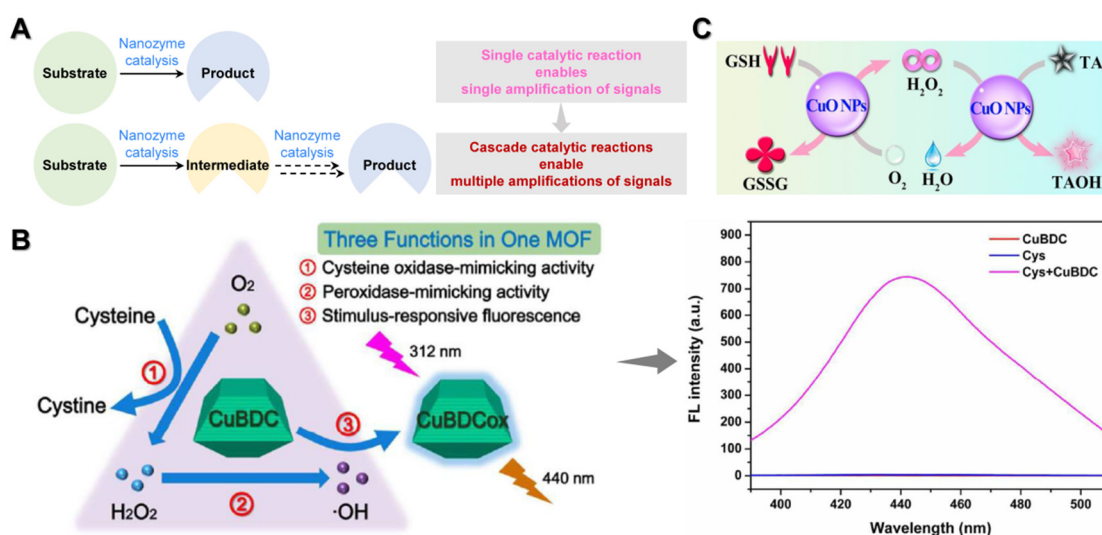


**Figure 3.** (A) Comparison of nanozyme-involved cascade catalytic reactions with a single reaction for highly-sensitive sensing. (B) Design of CuBDC with cascade cysteine oxidase- and peroxidase-mimicking activities for cysteine detection (reprinted with permission from Ref. [63]). (C) Self-cascade system based on CuO NPs with GSH oxidase- and peroxidase-like activities (reprinted with permission from Ref. [64]).

Similar enzyme-like activities were also found in CuO NPs by Liu's group [64]. The single-component CuO NPs not only acted as a glutathione (GSH) oxidase mimic, to oxidize GSH in the solution containing dissolved O<sub>2</sub>, where H<sub>2</sub>O<sub>2</sub> was produced, but also played a peroxidase-like role in inducing the oxidation of the TA substrate by the produced H<sub>2</sub>O<sub>2</sub>, with a high local concentration near CuO NPs. The dual enzyme-like activities of the Cu NPs produced a self-organized cascade reaction (Figure 3C), enabling the determination of GSH with good performance. By using the strong coordination interaction of GSH and metal ions, highly sensitive detection of Ag<sup>+</sup> was also achieved with the self-cascade nanozyme, providing a LOD down to 0.037 nM.

According to the above examples, the construction of self-cascade catalytic systems depends on the multi-activity features of a single nanozyme. Although, in recent years, increasing materials with more than one enzyme-mimetic activity have been explored to promote analytical applications, their use might also lead to some negative impacts [52]. For instance, both peroxidase- and oxidase-like activities are able to trigger the oxidation of substrates, even in the same environment. As a result, the oxidase-like catalytic reaction would affect the measurement of a target that originally relied only on the peroxidase-mimicking activity [46]. Therefore, more attention is required to rationally design nanozymes with the desired self-cascade catalytic activities, without introducing other irrelevant activities and interference.

### 3. Rational Design of Nanozymes to Improve Sensing Selectivity

Selectivity is another important parameter for a sensor. It is widely recognized that a lack of substrate specificity becomes the biggest challenge for nanozymes [26,68]. For this reason, foreign recognition elements are often utilized in combination with nanozymes to gain high-selectivity detection [14]. At present, a few means have been investigated to realize the above goal, such as constructing natural enzyme-nanozyme cascade sensors [51,69], combining nanozymes with DNA chains or aptamers [70–72], fabricating nanozyme-linked immunosensors [7], and utilizing the specific interactions between certain nanozymes and analytes [73,74]. To fundamentally solve the selectivity problem, rationally designing nanozymes that have intrinsic catalytic specificity is desirable. Here, structurally biomimetic nanozymes and molecularly imprinted nanozymes are discussed in detail, and their applications to achieve selective sensing are revealed.

#### 3.1. Structurally Biomimetic Nanozymes

It is known that the majority of natural enzymes are able to offer excellent substrate specificity. Such specificity mainly relies on their fine structures. In protein-based enzymes, complex multi-level structures provide clearly defined channels and cavities, with shape, size, and interactions well matching their corresponding substrates, thus endowing them with accurate substrate recognition and catalysis. Differently from bioenzymes, inorganic nanozyme materials inherently lack well-defined structures near active sites, leading to the very poor catalytic specificity of nanozymes. Naturally, the structural bionic concept inspires the design of nanozymes with surface microstructures similar to the corresponding bioenzymes [68], to obtain inorganic enzyme mimics with the desired catalytic selectivity.

In this regard, several studies on designing and developing nanozymes that mimic the fine structures of natural enzymes have been reported [75,76]. For instance, inspired by the active site structure of natural catechol oxidase, Li et al. fabricated a MOF material called MOF-818, which consisted of tri-nuclear copper centers (Figure 4A) [76]. In natural catechol oxidase (PDB code 1BT1), a six-histidine-coordinated binuclear Cu metal center plays the catalytic role in triggering the oxidation of *o*-diphenol. Correspondingly, the O<sub>2</sub> molecule was reduced to H<sub>2</sub>O<sub>2</sub> and further protonated via cleaving the HO–OH bond to generate H<sub>2</sub>O. Similarly, with tri-nuclear copper centers, MOF-818 could induce the catalytic oxidation of the substrate in the participation of dissolved O<sub>2</sub>, to finally generate H<sub>2</sub>O<sub>2</sub> instead of H<sub>2</sub>O. This was because the designed MOF-818 did not have a peroxidase-like activity. Unlike common CeO<sub>2</sub> and Pt NPs as nanozymes to induce the catalytic oxidation of

TMB or 2,2'-azino-bis(3-ethylbenzothiazoline-6-sulfonic acid) (ABTS) with the presence or absence of  $H_2O_2$ , the proposed MOF-818 only exhibited a catechol oxidase-mimetic activity to trigger the oxidation of 3,5-di-*tert*-butylcatechol (3,5-DTBC). As a consequence, the MOF-818 acting as a specific artificial catechol oxidase exhibited excellent catalytic selectivity.

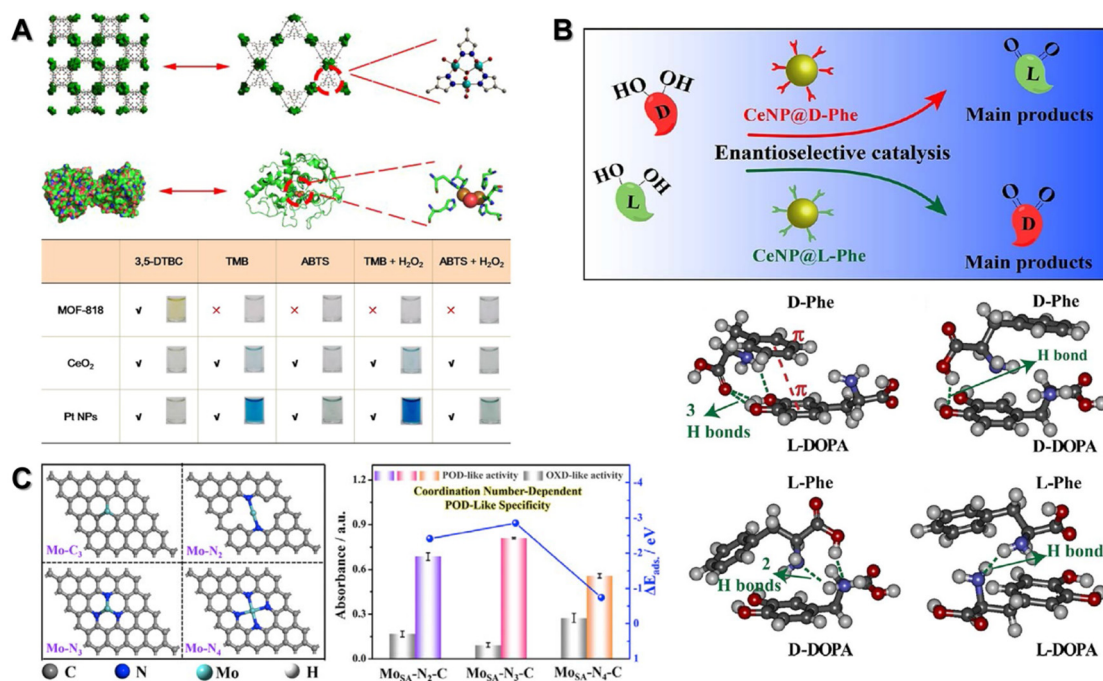


**Figure 4.** (A) Catechol oxidase-inspired design of MOF-818 showing a high catalytic specificity (reprinted with permission from Ref. [76]). (B) Chiral Phe-modified ceria nanoparticles as nanozymes for stereoselective catalysis (reprinted with permission from Ref. [77]). (C) Coordination number regulation of Mo-based SAN with peroxidase-like specificity (reprinted with permission from Ref. [78]).

As mentioned above, the fine surface structures near active centers play an important role in determining the selectivity of nanozymes toward substrates. This inspires the adjustment of the specificity of nanozymes by tailoring their surface. Typically, chiral catalysis can be obtained when some chiral ligands are anchored on an inorganic nanozyme surface [77,79–81]. In general, amino acid ligands and small chiral molecules, as well as DNA chains, are employed to modify the surface of inorganic materials to obtain chiral nanozymes. For example, Qu's group modified a series of D- or L-amino acids onto a ceria surface, to realize the enantioselective catalysis of 3,4-dihydroxyphenylalanine (DOPA) enantiomers [77], a commonly used drug for treating the Parkinson's disease. By measuring the reaction kinetics of ceria nanoparticles (CeNPs) decorated by eight different amino acids (phenylalanine, alanine, tryptophan, histidine, glutamic acid, arginine, lysine, and tyrosine), it was concluded that the phenylalanine (Phe)-coated CeNPs were optimal for DOPA oxidation and provided excellent stereoselectivity toward its enantiomers. In detail, L-Phe-decorated CeNPs offered a higher catalytic ability to oxidize D-DOPA, while D-Phe-decorated CeNPs were more effective toward L-DOPA (Figure 4B). Theoretical calculations indicated that both DOPA enantiomers could interact with the chiral Phe modifiers, mainly by forming different hydrogen bonds. Three hydrogen bonds could be formed between D-Phe and L-DOPA, compared to only one hydrogen bond formed between D-Phe and D-DOPA. Moreover, the  $\pi$ - $\pi$  aromatic packing interaction was able to further intensify the interaction of D-Phe and L-DOPA. On the contrary, in comparison with the interplay of L-Phe and L-DOPA, a stronger interaction could be obtained between L-Phe and D-DOPA by forming two hydrogen bonds. This indicated that the modification of chiral amino acids

on nanozyme surface could have a great impact on the stereoselectivity of the latter. These fascinating results are inspiring increasing efforts in designing chiral nanozymes [80].

Given SANs have clearly defined geometric and electronic structures and the microenvironment around active centers plays a significant role in determining their catalytic performance, one can tailor the microenvironment of SANs to obtain enhanced substrate selectivity [32]. As such, Wang et al. reported the development of several Mo-based SANs ( $\text{Mo}_{\text{SA}}\text{-N}_x\text{-C}$ ,  $x = 2, 3$  or  $4$ ) [78], and it was observed that their peroxidase-mimetic specificity could be adjusted by changing the coordination number of single-atom Mo sites. Compared to  $\text{Mo}_{\text{SA}}\text{-N}_2\text{-C}$  and  $\text{Mo}_{\text{SA}}\text{-N}_4\text{-C}$ , the optimized  $\text{Mo}_{\text{SA}}\text{-N}_3\text{-C}$  exhibited a significantly oppressed oxidase-like activity, but a higher peroxidase-mimicking activity was observed (Figure 4C). This study demonstrated the feasibility of rationally tailoring the microenvironment of SACs to obtain high-specificity nanozymes. Currently, although there have been very few cases of designing structurally biomimetic nanozymes for selective analysis, it is believed that in the near future the structural bionic concept will draw more and more attention to this topic.

### 3.2. Molecularly Imprinted Nanozymes

Molecularly imprinted polymers (MIPs) have artificial binding sites toward target molecules. They are generally synthesized via the co-polymerization of template molecules and functional monomers, with or without the addition of some cross-linking agents. After the template molecules are removed, some recognition cavities remain in the formed polymer matrix. The remaining cavities are complementary to the template molecules in shape, size, and chemical functional groups, and can selectively bind the template molecules again [82]. Combining MIPs with nanozymes provides a potential path to solve the poor substrate selectivity problem of the latter. For example, Zhang fabricated molecularly imprinted sites on peroxidase-like  $\text{Fe}_3\text{O}_4$  surface by utilizing the commonly used enzymatic substrates TMB and ABTS as template molecules [83]. In comparison with bare  $\text{Fe}_3\text{O}_4$  nanoparticles, the explored molecularly imprinted nanozymes presented improved catalytic kinetics toward the corresponding substrates. Importantly, the introduction of molecularly imprinted sites endowed the nanozyme with significantly enhanced specific affinities toward the substrates (Figure 5A). Similar phenomena have also been observed in other molecularly imprinted nanozymes [84–87]. These studies provide the basis of introducing artificial imprinting sites onto a nanozyme surface to solve the poor selectivity issue.

Instead of imprinting enzymatic substrates onto the nanozyme surface, one can use analytes as the template molecules and fabricate molecularly imprinted nanozymes for analytical applications [88–92]. As such, our group prepared molecularly imprinted sites on a peroxidase-mimetic  $\text{Fe}_3\text{O}_4$  nanoparticle surface through self-polymerizing dopamine (DA) in a weak alkaline environment [88], and further fabricated a colorimetric sensor for the high-selectivity determination of tetracycline (TC) (Figure 5B). The imprinted nanozyme ( $\text{Fe}_3\text{O}_4\text{@MIP}$ ) had abundant cavities and channels for substrates access to the peroxidase-like  $\text{Fe}_3\text{O}_4$  core. When TC was fed, it was selectively recognized and captured by the MIP shell and masked the cavities and channels. Consequently, the catalyzed TMB color reaction was suppressed. On the basis of such a principle, colorimetric sensing of TC with good selectivity against some structural analogues (oxytetracycline, chlorotetracycline, erythromycin, penicillin, et al.) was achieved. It should be stated that, although introducing molecular imprinting sites onto a nanozyme surface can improve the substrate specificity for selective detection, the imprinted layer introduced would significantly cover up the active surface and sites of nanozymes, thus leading to a decrease in catalytic activity. Thus, balancing the catalytic specificity and activity turns to be a vital issue. How to rationally design molecularly imprinted nanozymes with good specificity and enough activity for high-performance sensing is the current challenge.

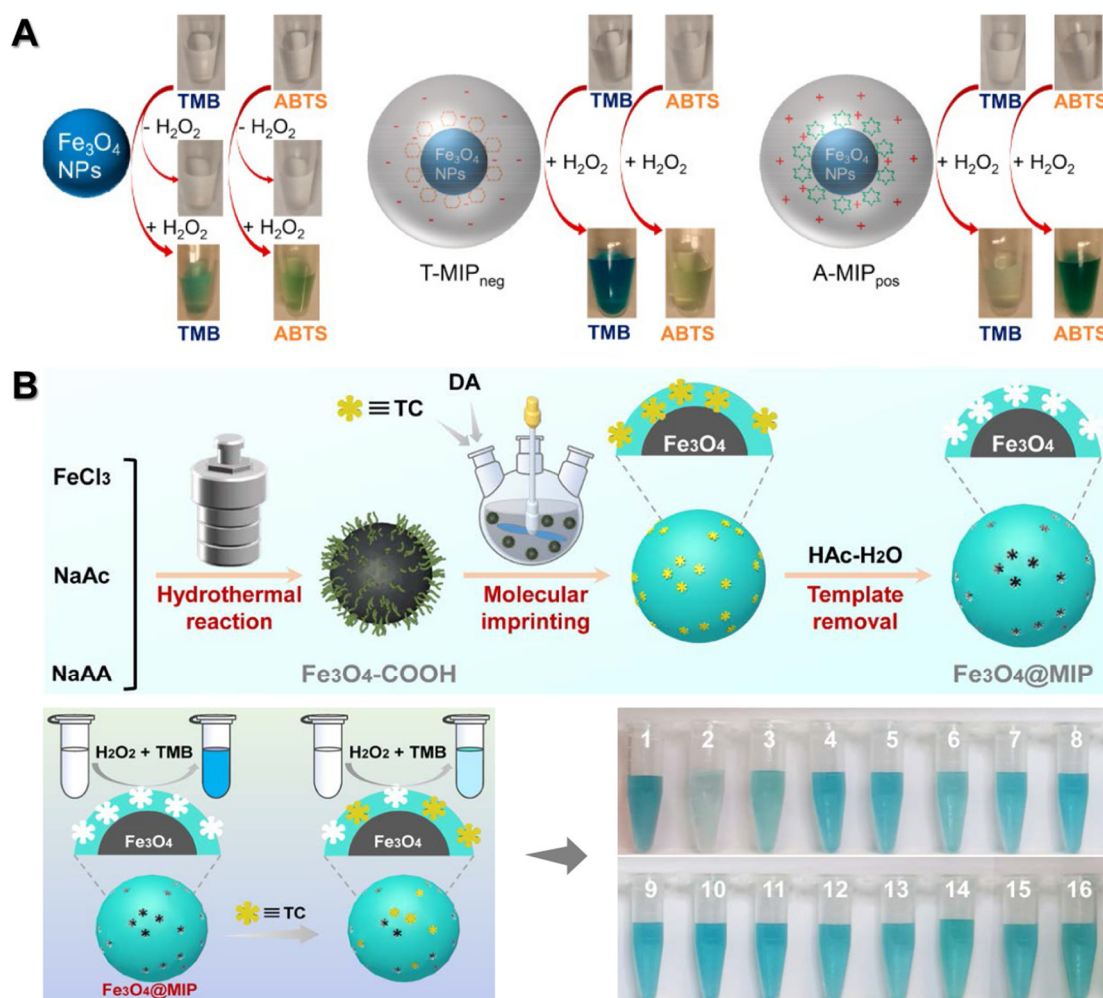


**Figure 5.** (A) Molecularly imprinted layers grown on  $\text{Fe}_3\text{O}_4$  NPs with substrate binding pockets for enhanced nanozyme specificity (reprinted with permission from Ref. [83]). (B) Molecular imprinting on  $\text{Fe}_3\text{O}_4$  particle surface to gain TC colorimetric detection with excellent selectivity (reprinted with permission from Ref. [88]).

#### 4. Rational Design of Nanozymes to Expand Application Scenarios

In addition to sensitivity and selectivity, expanding the application scenarios of nanozyme-based sensors is another research direction. This mainly includes how to design and develop nanozymes applicable to different environments, as well as how to realize high-performance detection using different sensing modes. Currently, although great progress has been made to serve the analytical sensing field, some intrinsic shortcomings still hinder the wide use of nanozymes. Here, we discuss the rational design of nanozymes that can break the pH limit and multifunctional nanozymes, both of which can greatly expand the applicability of enzyme mimics in analytical sensing.

##### 4.1. Nanozymes Breaking the pH Limit

To date, many materials have been explored as peroxidase-mimetic nanozymes, while the majority of them present their activity only in acidic conditions (pH 3.0–5.0). This is because in acidic media, the  $\text{H}_2\text{O}_2$  substrate prefers to undergo a homogeneous dissociation process to form hydroxyl radicals and trigger further reactions, thus exhibiting a peroxidase-like activity [93]. If the solution pH is expanded to the neutral medium, a very weak, or even no, activity is gained. This characteristic greatly limits the wider use of peroxidase mimics in biochemical analysis. Taking glucose detection as an example, two operation steps are often employed, where a peroxidase-like nanozyme is combined with natural

GOx. In detail, GOx is first used to trigger the oxidation of glucose in a neutral medium to produce  $H_2O_2$ , and the produced  $H_2O_2$  is then catalyzed by the peroxidase-like nanozyme in a moderately acidic medium, to trigger some chromogenic reactions. Obviously, such a two-step protocol results in some drawbacks: on the one hand, the  $H_2O_2$  species produced in the first step will spontaneously decompose, and its loss limits the detection sensitivity; on the other hand, different pH conditions are required for the bioenzyme–nanozyme cascade catalytic system, complicating the detection operation.

To solve the above dilemma, one can try to develop peroxidase-mimicking nanozymes that are able to exhibit the desired activity in physiological environments. To sum up, there mainly are two strategies used to expand the working pH of nanozymes (Figure 6A): one is to explore nanozymes with intrinsically high activity in acidic environments, which can also exhibit a certain activity in neutral media [94–99]; the other is to design the surface of nanozymes, where special surface engineering (introducing surface charge, fabricating acidic microenvironment, et al.) enables the extension of the working pH to neutral conditions [100–104].

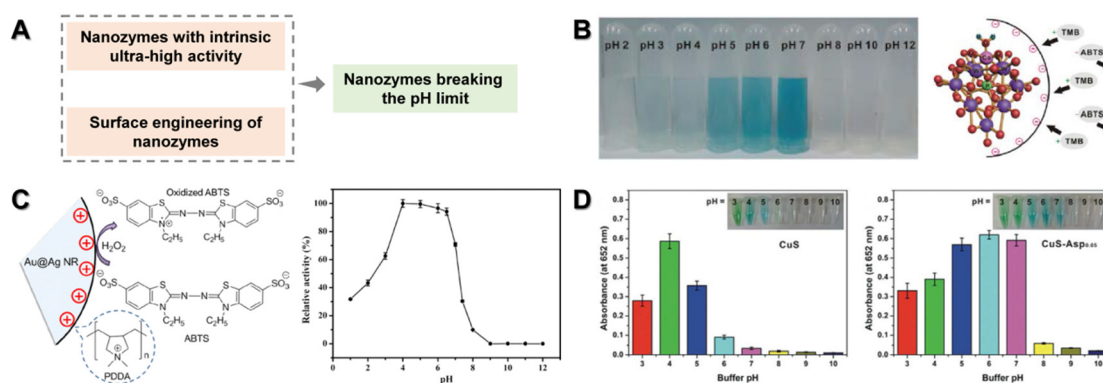


**Figure 6.** (A) Strategies to obtain nanozymes that can break the pH limit. (B) Co-based nanozyme showing good peroxidase-like activity in a neutral solution (reprinted with permission from Ref. [96]). (C) Au@Ag NRs modified with positively charged PDDA, showing a pH-dependent peroxidase-like activity (reprinted with permission from Ref. [101]). (D) Surface modification of nanoscale CuS with aspartic acid to gain favorable peroxidase-mimetic activity at neutral pH (reprinted with permission from Ref. [100]).

Thus, we designed a Co-based polyoxometalate nanozyme ( $CoPW_{11}O_{39}$ ) that could show good peroxidase-mimicking activity at neutral pH [96]. Zeta potential measurements indicated that the surface of the obtained  $CoPW_{11}O_{39}$  was negatively charged. As a result, it exhibited a strong ability to catalyze the oxidation of positively charged TMB, even under neutral conditions (Figure 6B). In contrast, no catalytic activity under the physiological conditions was found when negatively charged ABTS was used as the substrate. Given that the nanozyme and natural GOx had a similar working pH environment, they were used to develop a one-pot colorimetric method for glucose detection.

Another efficient strategy to modulate the working pH of peroxidase mimics is to modify charged ligands onto their surface. For example, Han et al. developed Au@Ag nanorods (NRs) stabilized by positively charged poly(diallyldimethylammonium) (PDDA), which exhibited a high activity level over a wide pH range (pH 4.0–6.5) when using ABTS as the chromogenic substrate (Figure 6C) [101]. At pH 6.5, the peroxidase-like activity of the Au@Ag NRs was stable, showing a strong affinity toward negatively charged ABTS. Given this character, the detection of  $H_2O_2$  at pH 6.5 was realized based on the PDDA-modified Au@Ag NRs catalyzing the colorimetric reaction of  $H_2O_2$  and ABTS. Similarly, we engineered the charge of peroxidase-mimetic CuS via amino acid surface modification, to achieve good catalytic activity in a neutral medium [100]. In detail, aspartic acid (Asp), an acidic amino acid with an isoelectric point of 2.97, was used to decorate the surface of CuS

during preparation. As the Asp modifier could be hydrolyzed to negatively charged species in the neutral condition, rich negative charges were observed on the nanozyme surface, which could prominently promote the diffusion and adsorption of the positively charged substrate TMB onto the active surface for reaction. As a consequence, differently from bare CuS that had little activity at neutral pH, the Asp modified CuS exhibited excellent peroxidase-mimetic activity in the same environment (Figure 6D). As an application of this, one-pot colorimetric determination of glucose was obtained by integrating GOx with the engineered peroxidase-mimetic nanozyme.

#### 4.2. Multifunctional Nanozymes

Intrinsically, nanozymes are a class of nanoscale materials. When the size of a material is conditioned to the nanometer level, a series of interesting properties emerge. In fact, apart from enzyme-like catalytic features, many materials also possess some attractive optical [105–107], magnetic [108–110], and electrical [111] properties or act as promising carriers [112–114] for biochemical analysis. These multiple properties of nanozymes offer biochemical sensing unparalleled benefits in practical applications. For instance, nanozymes with responsive fluorescence can be employed to self-output signals without introducing external substrates or labels. By combining the catalytic feature of nanozymes with their additional properties, multifunctional nanozymes have huge potential in the biochemical sensing area [115]. In this work, materials with both enzyme-like catalytic activity and luminescent properties are discussed.

Currently, several classes of materials with luminescent properties have been explored, including MOFs [116–127], coordination compounds [128,129], metal clusters [130], carbon dots [131,132], and  $C_3N_4$ -based materials [133]. These multifunctional nanozymes enable “turn-on” fluorescence, “turn-off” fluorescence, bimodal fluorescence/colorimetric, and ratiometric fluorescence measurements of analytes (Figure 7A). As a typical method, multifunctional nanozymes with fluorescent properties can be obtained by integrating TA with active metal nodes, to fabricate MOFs-based nanozymes, where TA acts as an organic ligand to bind  $Fe^{3+}$  or  $Cu^{2+}$  and exhibits a remarkable fluorescence when it is catalytically oxidized to TAOH. Thus, Ye’s group prepared a dual-functional MIL-53(Fe) material with peroxidase-like activity via the self-assembly of  $Fe^{3+}$  and TA, to enable the label-free “turn-on” fluorescence detection of  $H_2O_2$  and glucose [117]. Once  $H_2O_2$  was fed, the MIL-53(Fe) could provide a notable peroxidase-mimetic catalytic ability for decomposing  $H_2O_2$  to produce hydroxyl radicals, and the latter oxidized the ligand TA in the MIL-53(Fe) to TAOH, which presented a remarkable fluorescence at approximately 440 nm (Figure 7B). As a result, a self-reporting fluorescence sensor based on the MIL-53(Fe) was fabricated for  $H_2O_2$  sensing, free of the addition of any other substrate or label. By integrating the bi-functional nanozyme with GOx, convenient detection of glucose was also gained.

Recently, we designed a FeZr bimetal–organic framework material (UiO-66(Fe/Zr)- $NH_2$ ) with multiple roles (luminescent property, peroxidase-like activity, and target recognition) to construct a ratiometric fluorescence sensor for the high-performance sensing of phosphate ions (Pi) [119]. The employment of a fluorescent ligand (2-aminoterephthalic acid) made the MOF show a strong fluorescence at 435 nm (Figure 7C). The  $Fe^{3+}/Fe^{2+}$  nodes offered a good enzyme-mimicking ability for catalyzing the *o*-phenylenediamine (OPD) substrate to a fluorescent product (OPDox) at 555 nm, which could quench the fluorescence (435 nm) of UiO-66(Fe/Zr)- $NH_2$  because of the inner filter effect. The  $Zr^{4+}$  nodes in the material acted as sites for Pi recognition and capture. When Pi existed, it was specifically adsorbed onto the UiO-66(Fe/Zr)- $NH_2$  and decreased the latter’s peroxidase-mimicking activity. Consequently, the fluorescence of UiO-66(Fe/Zr)- $NH_2$  at 435 nm was restored, but the fluorescence at 555 nm was reduced. Based on the ratiometric sensing principle, efficient detection of Pi with favorable selectivity and sensitivity was gained. In another work, we developed a bimodal fluorescence/colorimetric approach for sensing pesticides, by coupling stimulus-triggered luminescence with oxidase-mimetic activity in Ce-based coordination polymer nanoparticles (CPNs(IV)) [128]. The CPNs(IV) offered

an oxidase-mimicking ability to catalyze the oxidation of colorless TMB to blue TMBox, offering a colorimetric signal at around 652 nm (Figure 7D); when ascorbic acid 2-phosphate (AAP) was utilized as an enzymatic substrate of acid phosphatase (ACP) to be hydrolyzed, the AA produced with a certain reducibility could induce the chemical reduction of  $Ce^{4+}$  in the CPNs(IV) to  $Ce^{3+}$ , leading to the production of CPNs(III). In comparison with CPNs(IV), the produced CPNs(III) exhibited a greatly reduced oxidase-mimicking activity, leading to a remarkable suppression of the TMB color reaction. In addition, the produced CPNs(III) offered a fluorescence peak at 356 nm; with the addition of OP or carbamate pesticides, the activity of ACP was inhibited. As a consequence, the hydrolytic procedure of AAP to AA was suppressed, and the conversion of CPNs(IV) to CPNs(III) was also blocked, thus resulting in the recovery of the TMB color reaction; however, the fluorescence signal of CPNs(III) was inhibited. On the basis of this sensing principle, bimodal fluorescence/colorimetric sensing of malathion, a typical OP, was demonstrated. In addition, the satisfactory interference-tolerance reliability and practicability of the method were confirmed.

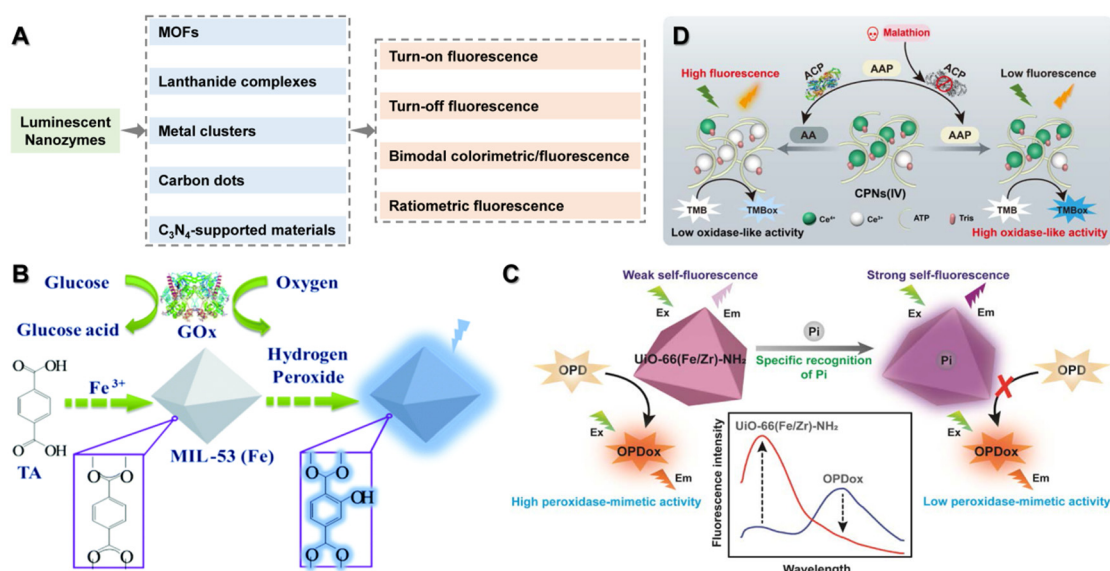


**Figure 7.** (A) Design of luminescent nanozymes for advanced fluorescence sensing. (B) Bifunctional MIL-53(Fe) nanozyme for label-free fluorescence detection of  $H_2O_2$  and glucose (reprinted with permission from Ref. [117]). (C) Design of UiO-66(Fe/Zr)-NH<sub>2</sub> enabling ratiometric fluorescence detection of Pi (reprinted with permission from Ref. [119]). (D) Bimodal colorimetric and fluorescence sensing of pesticides based on Ce-based coordination polymer nanoparticles with oxidase-like catalytic activity and stimulus-responsive luminescence (reprinted with permission from Ref. [128]).

## 5. Conclusions and Perspectives

Compared to natural bioenzymes, the attractive benefits of nanozymes have motivated the exploration of the abundant inorganic nanomaterials with enzyme-like properties, especially for sensing applications. On the other side of the coin, several obvious shortcomings have also been exposed in artificial enzyme mimics, including a low catalytic activity and poor substrate selectivity. To overcome these shortcomings and to better serve analytical sensing, the rational design of nanozymes is required. Great progress has been made in this field in the past few years. SANs with a comparable activity have been developed to provide higher sensitivity for nanozyme-based sensors. In addition, self-cascade nanozymes have been designed to fabricate tandem catalytic systems with multistage amplifications for ultrasensitive detection. For selective detection, some efficient strategies, including molecular imprinting and structurally bionic design, have been validated, to make up for the deficiency of catalytic specificity in nanozymes. Moreover, multifunctional nanozymes with luminescent properties, as well as nanozymes that can break the pH limit, have also

been applied in advanced analytical sensing. The design of these emerging nanozymes greatly promotes the creation of analytical principles, methods, technologies, and devices. Furthermore, an effectively enhanced analytical performance has been gained by using these nanozymes.

The trend of rationally designing nanozymes for biochemical detection is evident [134]. It is believed that in the near future more interesting nanozymes will be designed and developed, thus bringing extended methods and improved performance for biochemical sensing: (1) more material design strategies are expected to be explored to enhance the analytical performance of nanozyme-based sensors. The design concepts discussed above indeed solve some problems of the nanozymes used in analytical chemistry, while these are not sufficient to meet the increasing demands of modern measurement. As mentioned above, the nanozymes developed currently still have various challenges, including a low catalytic activity, poor substrate specificity, limited catalytic environment, and complex bioconjugation [135]. Thus, exploring new designs of nanozymes is necessary, to compensate for these shortcomings for advanced biochemical sensing. For instance, combining the bioenzyme-inspired design of SANs with the precise regulation of their active sites, as well as increasing the site density may be a promising way to improve the catalytic activity and specificity of nanozymes [46,78]. In order to further expand the applications of nanozymes, designing more nanozymes with multiple functions (e.g., nanozymes with fluorescent, chemiluminescent, Raman, magnetic, or/and electrical properties) is promising; (2) in addition to sensitivity, selectivity, and application scenarios, other analytical parameters should not be overlooked. Advanced sensing requires not only high selectivity, excellent selectivity, and good applicability, but also a rapid response, smart sensing, and simple operation. Although several nanozyme strategies have been demonstrated as efficient for enhancing the first three parameters, the improvement of response speed, detection operation, and smart sensing is still urgently needed, which requires future efforts from the community. For example, fabricating portable detection devices by integrating nanozyme sensing with 3D-printed accessories and smartphone-based sensing technology would enable the on-site rapid analysis of targets [136]. Ingenious integration of nanozymes and their reaction substrates, as well as other sensing elements (such as bioenzymes) in one carrier, makes it possible to simplify the detection operation [56]; (3) effective combination of nanozyme materials and analytical methods is expected. For a sensor, its analytical performance relies on both the sensing material used and the sensing principle and method. Only the rational combination of sensing materials and analytical methods will result in sensors with the desired detection performance. Therefore, more attention should be focused on integrating sensing methods with efficient nanozyme materials for better biochemical analysis, including exploring new nanozyme categories, developing new sensing modes, and expanding the detectable targets.

**Author Contributions:** Conceptualization, X.N.; methodology, J.L.; software, J.L.; resources, J.L., X.N.; writing—original draft preparation, J.L.; writing—review and editing, X.N. All authors have read and agreed to the published version of the manuscript.

**Funding:** This research received no external funding.

**Institutional Review Board Statement:** Not applicable.

**Informed Consent Statement:** Not applicable.

**Data Availability Statement:** Not applicable.

**Acknowledgments:** The authors would like to acknowledge the support from the Start-up Research Fund of University of South China. The work was also supported by the Faculty of Agricultural Equipment of Jiangsu University.

**Conflicts of Interest:** The authors declare no conflict of interest.

## Abbreviations

AA	Ascorbic acid
AAP	Ascorbic acid 2-phosphate
ABTS	2,2'-Azino-bis(3-ethylbenzothiazoline-6-sulfonic acid)
ACh	Acetylcholine
AChE	Acetylcholinesterase
ACP	Acid phosphatase
ALP	Alkaline phosphatase
Asp	Aspartic acid
BChE	Butyrylcholinesterase
CeNPs	Ceria nanoparticles
ChO	Choline oxidase
CNTs	Carbon nanotubes
CPNs(IV)	Ce-based coordination polymer nanoparticles
DA	Dopamine
DOPA	3,4-Dihydroxyphenylalanine
GOx	Glucose oxidase
GSH	Glutathione
HRP	Horseradish peroxidase
LOD	Limit of detection
MIPs	Molecularly imprinted polymers
MOFs	Metal-organic frameworks
OP	Organophosphorus
OPD	<i>o</i> -Phenylenediamine
PDDA	Poly(diallyldimethylammonium)
Phe	Phenylalanine
Pi	Phosphate ion
PPy	Polypyrrole
SACs	Single atomic catalysts
SANs	Single-atom nanozymes
TA	Terephthalic acid
TAOH	2-Hydroxyterephthalic acid
TC	Tetracycline
TMB	3,3',5,5'-Tetramethylbenzidine

## References

1. Wei, H.; Wang, E. Nanomaterials with Enzyme-like Characteristics (Nanozymes): Next-Generation Artificial Enzymes. *Chem. Soc. Rev.* **2013**, *42*, 6060–6093. [[CrossRef](#)] [[PubMed](#)]
2. Wei, H.; Gao, L.; Fan, K.; Liu, J.; He, J.; Qu, X.; Dong, S.; Wang, E.; Yan, X. Nanozymes: A clear definition with fuzzy edges. *Nano Today* **2021**, *40*, 101269. [[CrossRef](#)]
3. Liang, M.; Yan, X. Nanozymes: From new concepts, mechanisms, and standards to applications. *Acc. Chem. Res.* **2019**, *52*, 2190–2200. [[CrossRef](#)] [[PubMed](#)]
4. Jiao, J.; Fan, K.; Hu, Z.; Yan, X.; Du, P. Development trend and priority areas of nanozyme. *Sci. Sin. Chim.* **2019**, *49*, 1442–1453.
5. Ragg, R.; Tahir, M.N.; Tremel, W. Solids Go Bio: Inorganic Nanoparticles as Enzyme Mimics. *Eur. J. Inorg. Chem.* **2015**, *2016*, 1906–1915. [[CrossRef](#)]
6. Wang, Q.; Liu, S.; Tang, Z. Recent progress in the design of analytical methods based on nanozymes. *J. Mater. Chem. B* **2021**, *9*, 8174–8184. [[CrossRef](#)]
7. Niu, X.; Cheng, N.; Ruan, X.; Du, D.; Lin, Y. Review—Nanozyme-based immunosensors and immunoassays: Recent developments and future trends. *J. Electrochem. Soc.* **2020**, *167*, 037508. [[CrossRef](#)]
8. Wang, Q.; Wei, H.; Zhang, Z.; Wang, E.; Dong, S. Nanozyme: An emerging alternative to natural enzyme for biosensing and immunoassay. *TrAC Trends Anal. Chem.* **2018**, *105*, 218–224. [[CrossRef](#)]
9. Liu, B.; Liu, J. Surface modification of nanozymes. *Nano Res.* **2017**, *10*, 1125–1148. [[CrossRef](#)]
10. Li, X.; Wang, L.; Du, D.; Ni, L.; Pan, J.; Niu, X. Emerging applications of nanozymes in environmental analysis: Opportunities and trends. *TrAC Trends Anal. Chem.* **2019**, *120*, 115653. [[CrossRef](#)]
11. Song, W.; Zhao, B.; Wang, C.; Ozaki, Y.; Lu, X. Functional nanomaterials with unique enzyme-like characteristics for sensing applications. *J. Mater. Chem. B* **2019**, *7*, 850–875. [[CrossRef](#)]

12. Huang, L.; Sun, D.; Pu, H.; Wei, Q. Development of Nanozymes for Food Quality and Safety Detection: Principles and Recent Applications. *Compr. Rev. Food Sci. Food Saf.* **2019**, *18*, 1496–1513. [[CrossRef](#)]
13. Li, S.; Zhang, Y.; Wang, Q.; Lin, A.; Wei, H. Nanozyme-Enabled Analytical Chemistry. *Anal. Chem.* **2021**, *94*, 312–323. [[CrossRef](#)]
14. Li, X.; Zhu, H.; Liu, P.; Wang, M.; Pan, J.; Qiu, F.; Ni, L.; Niu, X. Realizing selective detection with nanozymes: Strategies and trends. *TrAC Trends Anal. Chem.* **2021**, *143*, 116379. [[CrossRef](#)]
15. Wang, H.; Wan, K.; Shi, X. Recent Advances in Nanozyme Research. *Adv. Mater.* **2019**, *31*, 1805368. [[CrossRef](#)]
16. Tian, Z.; Li, J.; Zhang, Z.; Gao, W.; Zhou, X.; Qu, Y. Highly sensitive and robust peroxidase-like activity of porous nanorods of ceria and their application for breast cancer detection. *Biomaterials* **2015**, *59*, 116–124. [[CrossRef](#)]
17. Shu, Q.W.; Li, C.M.; Gao, P.F.; Gao, M.X.; Huang, C.Z. Porous hollow CuS nanospheres with prominent peroxidase-like activity prepared in large scale by a one-pot controllable hydrothermal step. *RSC Adv.* **2015**, *5*, 17458–17465. [[CrossRef](#)]
18. Wu, H.; Liu, Y.; Li, M.; Chong, Y.; Zeng, M.; Lo, Y.M.; Yin, J.-J. Size-dependent tuning of horseradish peroxidase bioreactivity by gold nanoparticles. *Nanoscale* **2015**, *7*, 4505–4513. [[CrossRef](#)]
19. Xi, Z.; Gao, W.; Xia, X. Size effect in Pd–Ir core-shell nanoparticles as nanozymes. *ChemBioChem* **2020**, *21*, 2440–2444. [[CrossRef](#)]
20. Tang, G.; He, J.; Liu, J.; Yan, X.; Fan, K. Nanozyme for tumor therapy: Surface modification matters. *Exploration* **2021**, *1*, 75–89. [[CrossRef](#)]
21. Jampaiah, D.; Reddy, T.S.; Kandjani, A.E.; Selvakannan, P.R.; Sabri, Y.M.; Coyle, V.E.; Shukla, R.; Bhargava, S.K. Fe-doped CeO<sub>2</sub> nanorods for enhanced peroxidase-like activity and their application towards glucose detection. *J. Mater. Chem. B* **2016**, *4*, 3874–3885. [[CrossRef](#)]
22. Gao, M.; Lu, X.; Chen, S.; Tian, D.; Zhu, Y.; Wang, C. Enhanced peroxidase-like activity of Mo<sup>6+</sup>-doped Co<sub>3</sub>O<sub>4</sub> nanotubes for ultrasensitive and colorimetric L-cysteine detection. *ACS Appl. Nano Mater.* **2018**, *1*, 4703–4715. [[CrossRef](#)]
23. Nagvenkar, A.P.; Gedanken, A. Cu<sub>0.89</sub>Zn<sub>0.11</sub>O, A New Peroxidase-Mimicking Nanozyme with High Sensitivity for Glucose and Antioxidant Detection. *ACS Appl. Mater. Interfaces* **2016**, *8*, 22301–22308. [[CrossRef](#)] [[PubMed](#)]
24. Liu, M.; Zhao, H.; Chen, S.; Yu, H.; Quan, X. Stimuli-responsive peroxidase mimicking at a smart graphene interface. *Chem. Commun.* **2012**, *48*, 7055–7057. [[CrossRef](#)] [[PubMed](#)]
25. Huang, Y.; Ren, J.; Qu, X. Nanozymes: Classification, Catalytic Mechanisms, Activity Regulation, and Applications. *Chem. Rev.* **2019**, *119*, 4357–4412. [[CrossRef](#)] [[PubMed](#)]
26. Wu, J.; Wang, X.; Wang, Q.; Lou, Z.; Li, S.; Zhu, Y.; Qin, L.; Wei, H. Nanomaterials with enzyme-like characteristics (nanozymes): Next-generation artificial enzymes (II). *Chem. Soc. Rev.* **2018**, *48*, 1004–1076. [[CrossRef](#)] [[PubMed](#)]
27. Qiao, B.; Wang, A.; Yang, X.; Allard, L.F.; Jiang, Z.; Cui, Y.; Liu, J.; Li, J.; Zhang, T. Single-atom catalysis of CO oxidation using Pt<sub>1</sub>/FeO<sub>x</sub>. *Nat. Chem.* **2011**, *3*, 634–641. [[CrossRef](#)]
28. Wang, A.; Li, J.; Zhang, T. Heterogeneous single-atom catalysis. *Nat. Rev. Chem.* **2018**, *2*, 65–81. [[CrossRef](#)]
29. Kaiser, S.K.; Chen, Z.; Akl, D.F.; Mitchell, S.; Pérez-Ramírez, J. Single-Atom Catalysts across the Periodic Table. *Chem. Rev.* **2020**, *120*, 11703–11809. [[CrossRef](#)]
30. Jiao, L.; Yan, H.; Wu, Y.; Gu, W.; Zhu, C.; Du, D.; Lin, Y. When Nanozymes Meet Single-Atom Catalysis. *Angew. Chem. Int. Ed.* **2019**, *59*, 2565–2576. [[CrossRef](#)]
31. Ding, S.; Lyu, Z.; Fang, L.; Li, T.; Zhu, W.; Li, S.; Li, X.; Li, J.C.; Du, D.; Lin, Y. Single-atomic site catalyst with heme enzymes-like active sites for electrochemical sensing of hydrogen peroxide. *Small* **2021**, *17*, 2100664. [[CrossRef](#)]
32. Wu, W.; Huang, L.; Wang, E.; Dong, S. Atomic engineering of single-atom nanozymes for enzyme-like catalysis. *Chem. Sci.* **2020**, *11*, 9741–9756. [[CrossRef](#)]
33. Zhao, C.; Xiong, C.; Liu, X.; Qiao, M.; Li, Z.; Yuan, T.; Wang, J.; Qu, Y.; Wang, X.; Zhou, F.; et al. Unraveling the enzyme-like activity of heterogeneous single atom catalyst. *Chem. Commun.* **2019**, *55*, 2285–2288. [[CrossRef](#)]
34. Ma, W.; Mao, J.; Yang, X.; Pan, C.; Chen, W.; Wang, M.; Yu, P.; Mao, L.; Li, Y. A single-atom Fe–N<sub>4</sub> catalytic site mimicking bi-functional antioxidative enzymes for oxidative stress cytoprotection. *Chem. Commun.* **2019**, *55*, 159–162. [[CrossRef](#)]
35. Li, X.; Liu, L.; Ren, X.; Gao, J.; Huang, Y.; Liu, B. Microenvironment modulation of single-atom catalysts and their roles in electrochemical energy conversion. *Sci. Adv.* **2020**, *6*, eabb6833. [[CrossRef](#)]
36. Xu, B.; Wang, H.; Wang, W.; Gao, L.; Li, S.; Pan, X.; Wang, H.; Yang, H.; Meng, X.; Wu, Q.; et al. A Single-Atom Nanozyme for Wound Disinfection Applications. *Angew. Chem. Int. Ed.* **2019**, *58*, 4911–4916. [[CrossRef](#)]
37. Huang, L.; Chen, J.; Gan, L.; Wang, J.; Dong, S. Single-atom nanozymes. *Sci. Adv.* **2019**, *5*, eaav5490. [[CrossRef](#)]
38. Ji, S.; Jiang, B.; Hao, H.; Chen, Y.; Dong, J.; Mao, Y.; Zhang, Z.; Gao, R.; Chen, W.; Zhang, R.; et al. Matching the kinetics of natural enzymes with a single-atom iron nanozyme. *Nat. Catal.* **2021**, *4*, 407–417. [[CrossRef](#)]
39. Lin, S.; Wei, H. Design of high performance nanozymes: A single-atom strategy. *Sci. China Life Sci.* **2019**, *62*, 710–712. [[CrossRef](#)]
40. Jin, H.; Ye, D.; Shen, L.; Fu, R.; Tang, Y.; Jung, J.C.-Y.; Zhao, H.; Zhang, J. Perspective for Single Atom Nanozymes Based Sensors: Advanced Materials, Sensing Mechanism, Selectivity Regulation, and Applications. *Anal. Chem.* **2022**, *94*, 1499–1509. [[CrossRef](#)]
41. Cheng, N.; Li, J.C.; Liu, D.; Lin, Y.; Du, D. Single-atom nanozyme based on nanoengineered Fe–N–C catalyst with superior peroxidase-like activity for ultrasensitive bioassays. *Small* **2019**, *15*, 1901485. [[CrossRef](#)]
42. Wu, Y.; Jiao, L.; Luo, X.; Xu, W.; Wei, X.; Wang, H.; Yan, H.; Gu, W.; Xu, B.Z.; Du, D.; et al. Oxidase-like Fe–N–C single-atom nanozymes for the detection of acetylcholinesterase activity. *Small* **2019**, *15*, 1903108. [[CrossRef](#)]

43. Lyu, Z.; Ding, S.; Zhang, N.; Zhou, Y.; Cheng, N.; Wang, M.; Xu, M.; Feng, Z.; Niu, X.; Cheng, Y.; et al. Single-atom nanozymes linked immunosorbent assay for sensitive detection of A $\beta$  1-40: A biomarker of Alzheimer's disease. *Research* **2020**, *2020*, 4724505. [[CrossRef](#)]
44. Niu, X.; Shi, Q.; Zhu, W.; Liu, D.; Tian, H.; Fu, S.; Cheng, N.; Li, S.; Smith, J.N.; Du, D.; et al. Unprecedented peroxidase-mimicking activity of single-atom nanozyme with atomically dispersed Fe–N<sub>x</sub> moieties hosted by MOF derived porous carbon. *Biosens. Bioelectron.* **2019**, *142*, 111495. [[CrossRef](#)]
45. Chen, Q.; Li, S.; Liu, Y.; Zhang, X.; Tang, Y.; Chai, H.; Huang, Y. Size-controllable Fe-N/C single-atom nanozyme with exceptional oxidase-like activity for sensitive detection of alkaline phosphatase. *Sensors Actuators B Chem.* **2019**, *305*, 127511. [[CrossRef](#)]
46. Wu, Y.; Wu, J.; Jiao, L.; Xu, W.; Wang, H.; Wei, X.; Gu, W.; Ren, G.; Zhang, N.; Zhang, Q.; et al. Cascade Reaction System Integrating Single-Atom Nanozymes with Abundant Cu Sites for Enhanced Biosensing. *Anal. Chem.* **2020**, *92*, 3373–3379. [[CrossRef](#)]
47. Wang, D.; Zhao, Y. Single-atom engineering of metal-organic frameworks toward healthcare. *Chem* **2021**, *7*, 2635–2671. [[CrossRef](#)]
48. Jiang, B.; Duan, D.; Gao, L.; Zhou, M.; Fan, K.; Tang, Y.; Xi, J.; Bi, Y.; Tong, Z.; Gao, G.F.; et al. Standardized assays for determining the catalytic activity and kinetics of peroxidase-like nanozymes. *Nat. Protoc.* **2018**, *13*, 1506–1520. [[CrossRef](#)]
49. Wu, J.; Xiong, L.; Zhao, B.; Liu, M.; Huang, L. Densely Populated Single Atom Catalysts. *Small Methods* **2019**, *4*, 2106139. [[CrossRef](#)]
50. Zhang, X.; Li, G.; Chen, G.; Wu, D.; Wu, Y.; James, T.D. Enzyme Mimics for Engineered Biomimetic Cascade Nanoreactors: Mechanism, Applications, and Prospects. *Adv. Funct. Mater.* **2021**, *31*, 2106139. [[CrossRef](#)]
51. Cai, X.; Jiao, L.; Yan, H.; Wu, Y.; Gu, W.; Du, D.; Lin, Y.; Zhu, C. Nanozyme-involved biomimetic cascade catalysis for biomedical applications. *Mater. Today* **2021**, *44*, 211–228. [[CrossRef](#)]
52. Niu, X.; Liu, B.; Hu, P.; Zhu, H.; Wang, M. Nanozymes with Multiple Activities: Prospects in Analytical Sensing. *Biosensors* **2022**, *12*, 251. [[CrossRef](#)] [[PubMed](#)]
53. Ma, Y.; Tian, Z.; Zhai, W.; Qu, Y. Insights on catalytic mechanism of CeO<sub>2</sub> as multiple nanozymes. *Nano Res.* **2022**, 1–15. [[CrossRef](#)] [[PubMed](#)]
54. Guo, S.; Guo, L. Unraveling the Multi-Enzyme-Like Activities of Iron Oxide Nanozyme via a First-Principles Microkinetic Study. *J. Phys. Chem. C* **2019**, *123*, 30318–30334. [[CrossRef](#)]
55. Liu, J.; Zhang, W.; Peng, M.; Ren, G.; Guan, L.; Li, K.; Lin, Y. ZIF-67 as a template generating and tuning “raisin pudding”-type nanozymes with multiple enzyme-like activities: Toward online electrochemical detection of 3,4-dihydroxyphenylacetic acid in living brains. *ACS Appl. Mater. Interfaces* **2020**, *12*, 29631–29640. [[CrossRef](#)] [[PubMed](#)]
56. Zhu, H.; Xu, L.; Hu, P.; Liu, B.; Wang, M.; Yin, X.; Pan, J.; Niu, X. Smartphone-assisted bioenzyme-nanozyme-chromogen all-in-one test strip with enhanced cascade signal amplification for convenient paraoxon sensing. *Biosens. Bioelectron.* **2022**, *215*, 114583. [[CrossRef](#)]
57. Sengupta, P.; Pramanik, K.; Datta, P.; Sarkar, P. Chemically modified carbon nitride-chitin-acetic acid hybrid as a metal-free bifunctional nanozyme cascade of glucose oxidase-peroxidase for “click off” colorimetric detection of peroxide and glucose. *Biosens. Bioelectron.* **2020**, *154*, 112072. [[CrossRef](#)]
58. Lin, A.; Sun, Z.; Xu, X.; Zhao, S.; Li, J.; Sun, H.; Wang, Q.; Jiang, Q.; Wei, H.; Shi, D. Self-Cascade Uricase/Catalase Mimics Alleviate Acute Gout. *Nano Lett.* **2021**, *22*, 508–516. [[CrossRef](#)]
59. Meng, X.; Li, D.; Chen, L.; He, H.; Wang, Q.; Hong, C.; He, J.; Gao, X.; Yang, Y.; Jiang, B.; et al. High-Performance Self-Cascade Pyrite Nanozymes for Apoptosis–Ferroptosis Synergistic Tumor Therapy. *ACS Nano* **2021**, *15*, 5735–5751. [[CrossRef](#)]
60. Tao, N.; Li, H.; Deng, L.; Zhao, S.; Ouyang, J.; Wen, M.; Chen, W.; Zeng, K.; Wei, C.; Liu, Y.-N. A Cascade Nanozyme with Amplified Sonodynamic Therapeutic Effects through Comodulation of Hypoxia and Immunosuppression against Cancer. *ACS Nano* **2021**, *16*, 485–501. [[CrossRef](#)]
61. Wang, Q.; Cheng, C.; Zhao, S.; Liu, Q.; Zhang, Y.; Liu, W.; Zhao, X.; Zhang, H.; Pu, J.; Zhang, S.; et al. A valence-engineered self-cascading antioxidant nanozyme for the therapy of inflammatory bowel disease. *Angew. Chem. Int. Ed.* **2022**, *61*, e202201101.
62. Zhang, X.; Zhang, S.; Yang, Z.; Wang, Z.; Tian, X.; Zhou, R. Self-cascade MoS<sub>2</sub> nanozymes for efficient intracellular antioxidation and hepatic fibrosis therapy. *Nanoscale* **2021**, *13*, 12613–12622. [[CrossRef](#)]
63. Li, X.; Zhou, H.; Qi, F.; Niu, X.; Xu, X.; Qiu, F.; He, Y.; Pan, J.; Ni, L. Three hidden talents in one framework: A terephthalic acid-coordinated cupric metal–organic framework with cascade cysteine oxidase- and peroxidase-mimicking activities and stimulus-responsive fluorescence for cysteine sensing. *J. Mater. Chem. B* **2018**, *6*, 6207–6211. [[CrossRef](#)]
64. He, L.; Lu, Y.; Gao, X.; Song, P.; Huang, Z.; Liu, S.; Liu, Y. Self-cascade system based on cupric oxide nanoparticles as dual-functional enzyme mimics for ultrasensitive detection of silver ions. *ACS Sustain. Chem. Eng.* **2018**, *6*, 12132–12139. [[CrossRef](#)]
65. Chen, L.F.; Lin, M.T.; Noreldeen, H.A.A.; Peng, H.P.; Deng, H.H.; He, S.B.; Chen, W. Fructose oxidase-like activity of CuO nanoparticles supported by phosphate for a tandem catalysis-based fructose sensor. *Anal. Chim. Acta* **2022**, *1220*, 340064. [[CrossRef](#)]
66. He, S.-B.; Balasubramanian, P.; Hu, A.-L.; Zheng, X.-Q.; Lin, M.-T.; Xiao, M.-X.; Peng, H.-P.; Deng, H.-H.; Chen, W. One-pot cascade catalysis at neutral pH driven by CuO tandem nanozyme for ascorbic acid and alkaline phosphatase detection. *Sens. Actuators B Chem.* **2020**, *321*, 128511. [[CrossRef](#)]
67. Liu, Y.; Jin, H.; Zou, W.; Guo, R. Protein-mediated wool-ball-like copper sulfide as a multifunctional nanozyme for dual fluorescence “turn-on” sensors of cysteine and silver ions. *J. Mater. Chem. B* **2020**, *8*, 9075–9083. [[CrossRef](#)]

68. Wang, Z.; Zhang, R.; Yan, X.; Fan, K. Structure and activity of nanozymes: Inspirations for *de novo* design of nanozymes. *Mater. Today* **2020**, *41*, 81–119. [[CrossRef](#)]
69. Wei, H.; Wang, E. Fe<sub>3</sub>O<sub>4</sub> magnetic nanoparticles as peroxidase mimetics and their applications in H<sub>2</sub>O<sub>2</sub> and glucose detection. *Anal. Chem.* **2008**, *80*, 2250–2254. [[CrossRef](#)]
70. Wang, C.; Tang, G.; Tan, H. Colorimetric determination of mercury(II) via the inhibition by ssDNA of the oxidase-like activity of a mixed valence state cerium-based metal-organic framework. *Mikrochim. Acta* **2018**, *185*, 475. [[CrossRef](#)]
71. Weerathunge, P.; Ramanathan, R.; Shukla, R.; Sharma, T.K.; Bansal, V. Aptamer-Controlled Reversible Inhibition of Gold Nanozyme Activity for Pesticide Sensing. *Anal. Chem.* **2014**, *86*, 11937–11941. [[CrossRef](#)]
72. Li, S.; Zhao, X.; Yu, X.; Wan, Y.; Yin, M.; Zhang, W.; Cao, B.; Wang, H. Fe<sub>3</sub>O<sub>4</sub> nanozymes with aptamer-tuned catalysis for selective colorimetric analysis of ATP in blood. *Anal. Chem.* **2019**, *91*, 14737–14742. [[CrossRef](#)]
73. Liu, B.; Huang, Z.; Liu, J. Boosting the oxidase mimicking activity of nanoceria by fluoride capping: Rivaling protein enzymes and ultrasensitive F<sup>−</sup> detection. *Nanoscale* **2016**, *8*, 13562–13567. [[CrossRef](#)] [[PubMed](#)]
74. Long, Y.J.; Li, Y.F.; Liu, Y.; Zheng, J.J.; Tang, J.; Huang, C.Z. Visual observation of the mercury-stimulated peroxidase mimetic activity of gold nanoparticles. *Chem. Commun.* **2011**, *47*, 11939–11941. [[CrossRef](#)]
75. Chen, J.; Huang, L.; Wang, Q.; Wu, W.; Zhang, H.; Fang, Y.; Dong, S. Bio-inspired nanozyme: A hydratase mimic in a zeolitic imidazolate framework. *Nanoscale* **2019**, *11*, 5960–5966. [[CrossRef](#)]
76. Li, M.; Chen, J.; Wu, W.; Fang, Y.; Dong, S. Oxidase-like MOF-818 nanozyme with high specificity for catalysis of catechol oxidation. *J. Am. Chem. Soc.* **2020**, *142*, 15569–15574. [[CrossRef](#)]
77. Sun, Y.; Zhao, C.; Gao, N.; Ren, J.; Qu, X. Stereoselective Nanozyme Based on Ceria Nanoparticles Engineered with Amino Acids. *Chem.–A Eur. J.* **2017**, *23*, 18146–18150. [[CrossRef](#)]
78. Wang, Y.; Jia, G.; Cui, X.; Zhao, X.; Zhang, Q.; Gu, L.; Zheng, L.; Li, L.H.; Wu, Q.; Singh, D.J.; et al. Coordination Number Regulation of Molybdenum Single-Atom Nanozyme Peroxidase-like Specificity. *Chem* **2020**, *7*, 436–449. [[CrossRef](#)]
79. Zhou, Y.; Wei, Y.; Ren, J.; Qu, X. A chiral covalent organic framework (COF) nanozyme with ultrahigh enzymatic activity. *Mater. Horizons* **2020**, *7*, 3291–3297. [[CrossRef](#)]
80. Zhang, R.; Zhou, Y.; Yan, X.; Fan, K. Advances in chiral nanozymes: A review. *Microchim. Acta* **2019**, *186*, 782. [[CrossRef](#)] [[PubMed](#)]
81. Dong, K.; Xu, C.; Ren, J.; Qu, X. Chiral Nanozymes for Enantioselective Biological Catalysis. *Angew. Chem. Int. Ed.* **2022**. [[CrossRef](#)]
82. BelBruno, J.J. Molecularly imprinted polymers. *Chem. Rev.* **2019**, *119*, 94–119. [[CrossRef](#)] [[PubMed](#)]
83. Zhang, Z.; Zhang, X.; Liu, B.; Liu, J. Molecular Imprinting on Inorganic Nanozymes for Hundred-fold Enzyme Specificity. *J. Am. Chem. Soc.* **2017**, *139*, 5412–5419. [[CrossRef](#)] [[PubMed](#)]
84. Zhang, Z.; Liu, J. Intracellular delivery of a molecularly imprinted peroxidase mimicking DNAzyme for selective oxidation. *Mater. Horizons* **2018**, *5*, 738–744. [[CrossRef](#)]
85. Zhang, Z.; Liu, B.; Liu, J. Molecular Imprinting for Substrate Selectivity and Enhanced Activity of Enzyme Mimics. *Small* **2016**, *13*, 1602730. [[CrossRef](#)]
86. Zhang, Z.; Li, Y.; Zhang, X.; Liu, J. Molecularly imprinted nanozymes with faster catalytic activity and better specificity. *Nanoscale* **2019**, *11*, 4854–4863. [[CrossRef](#)]
87. Zhang, Z.; Liu, Y.; Zhang, X.; Liu, J. A Cell-Mimicking Structure Converting Analog Volume Changes to Digital Colorimetric Output with Molecular Selectivity. *Nano Lett.* **2017**, *17*, 7926–7931. [[CrossRef](#)]
88. Liu, B.; Zhu, H.; Feng, R.; Wang, M.; Hu, P.; Pan, J.; Niu, X. Facile Molecular Imprinting on Magnetic Nanozyme Surface for Highly Selective Colorimetric Detection of Tetracycline. *Sens. Actuators B Chem.* **2022**, *370*, 132451. [[CrossRef](#)]
89. Fan, L.; Lou, D.; Wu, H.; Zhang, X.; Zhu, Y.; Gu, N.; Zhang, Y. A novel AuNP-based glucose oxidase mimic with enhanced activity and selectivity constructed by molecular imprinting and O<sub>2</sub>-containing nanoemulsion embedding. *Adv. Mater. Interfaces* **2018**, *5*, 1801070. [[CrossRef](#)]
90. Wu, Y.; Chen, Q.; Liu, S.; Xiao, H.; Zhang, M.; Zhang, X. Surface molecular imprinting on g-C<sub>3</sub>N<sub>4</sub> photooxidative nanozyme for improved colorimetric biosensing. *Chin. Chem. Lett.* **2019**, *30*, 2186–2190. [[CrossRef](#)]
91. Zhang, Y.; Feng, Y.S.; Ren, X.H.; He, X.W.; Li, W.Y.; Zhang, Y.K. Bimetallic molecularly imprinted nanozyme: Dual-mode detection platform. *Biosens. Bioelectron.* **2022**, *196*, 113718. [[CrossRef](#)]
92. Cardoso, A.R.; Frasco, M.F.; Serrano, V.; Fortunato, E.; Sales, M.G.F. Molecular imprinting on nanozymes for sensing applications. *Biosensors* **2021**, *11*, 152. [[CrossRef](#)]
93. Li, J.; Liu, W.; Wu, X.; Gao, X. Mechanism of pH-switchable peroxidase and catalase-like activities of gold, silver, platinum and palladium. *Biomaterials* **2015**, *48*, 37–44. [[CrossRef](#)]
94. Zhang, J.; Wang, J.; Liao, J.; Lin, Y.; Zheng, C.; Liu, J. In Situ Fabrication of Nanoceria with Oxidase-like Activity at Neutral pH: Mechanism and Boosted Bio-Nanozyme Cascades. *ACS Appl. Mater. Interfaces* **2021**, *13*, 50236–50245. [[CrossRef](#)]
95. Zhang, J.; Wu, S.; Lu, X.; Wu, P.; Liu, J. Manganese as a Catalytic Mediator for Photo-oxidation and Breaking the pH Limitation of Nanozymes. *Nano Lett.* **2019**, *19*, 3214–3220. [[CrossRef](#)]
96. He, Y.; Li, X.; Xu, X.; Pan, J.; Niu, X. A cobalt-based polyoxometalate nanozyme with high peroxidase-mimicking activity at neutral pH for one-pot colorimetric analysis of glucose. *J. Mater. Chem. B* **2018**, *6*, 5750–5755. [[CrossRef](#)]

97. Li, D.; Guo, Q.; Ding, L.; Zhang, W.; Cheng, L.; Wang, Y.; Xu, Z.; Wang, H.; Gao, L. Bimetallic CuCo<sub>2</sub>S<sub>4</sub> nanozymes with enhanced peroxidase activity at neutral pH for combating burn infections. *ChemBioChem* **2020**, *21*, 2620–2627. [[CrossRef](#)]
98. Nguyen, P.T.; Lee, J.; Cho, A.; Kim, M.S.; Choi, D.; Han, J.W.; Kim, M.I.; Lee, J. Rational development of Co-doped mesoporous ceria with high peroxidase-mimicking activity at neutral pH for paper-based colorimetric detection of multiple biomarkers. *Adv. Funct. Mater.* **2022**, *32*, 2112428. [[CrossRef](#)]
99. Zhu, Q.; Yang, J.; Peng, Z.; He, Z.; Chen, W.; Tang, H.; Li, Y. Selective detection of glutathione by flower-like NiV<sub>2</sub>O<sub>6</sub> with only peroxidase-like activity at neutral pH. *Talanta* **2021**, *234*, 122645. [[CrossRef](#)]
100. Niu, X.; Xu, X.; Li, X.; Pan, J.; Qiu, F.; Zhao, H.; Lan, M. Surface charge engineering of nanosized CuS via acidic amino acid modification enables high peroxidase-mimicking activity at neutral pH for one-pot detection of glucose. *Chem. Commun.* **2018**, *54*, 13443–13446. [[CrossRef](#)]
101. Han, L.; Li, C.; Zhang, T.; Lang, Q.; Liu, A. Au@Ag Heterogeneous Nanorods as Nanozyme Interfaces with Peroxidase-Like Activity and Their Application for One-Pot Analysis of Glucose at Nearly Neutral pH. *ACS Appl. Mater. Interfaces* **2015**, *7*, 14463–14470. [[CrossRef](#)]
102. Chen, Q.; Liu, Y.; Liu, J.; Liu, J. Liposome-boosted peroxidase-mimicking nanozymes breaking the pH limit. *Chem. Eur. J.* **2020**, *26*, 16659–16665. [[CrossRef](#)]
103. Gu, H.; Huang, Q.; Zhang, J.; Li, W.; Fu, Y. Heparin as a bifunctional biotemplate for Pt nanocluster with exclusively peroxidase mimicking activity at near-neutral pH. *Colloids Surf. A Physicochem. Eng. Asp.* **2020**, *606*. [[CrossRef](#)]
104. Yin, X.; Liu, P.; Xu, X.; Pan, J.; Li, X.; Niu, X. Breaking the pH limitation of peroxidase-like CoFe<sub>2</sub>O<sub>4</sub> nanozyme via vitrification for one-step glucose detection at physiological pH. *Sens. Actuators B Chem.* **2020**, *328*, 129033. [[CrossRef](#)]
105. Wang, L.; Chen, Y. Luminescence-Sensing Tb-MOF Nanozyme for the Detection and Degradation of Estrogen Endocrine Disruptors. *ACS Appl. Mater. Interfaces* **2020**, *12*, 8351–8358. [[CrossRef](#)]
106. Wu, J.; Qin, K.; Yuan, D.; Tan, J.; Qin, L.; Zhang, X.; Wei, H. Rational design of Au@Pt multibranching nanostructures as bi-functional nanozymes. *ACS Appl. Mater. Interfaces* **2018**, *10*, 12954–12959. [[CrossRef](#)]
107. Zhu, N.; Gu, L.; Wang, J.; Li, X.; Liang, G.-X.; Zhou, J.; Zhang, Z. Novel and Sensitive Chemiluminescence Sensors Based on 2D-MOF Nanosheets for One-Step Detection of Glucose in Human Urine. *J. Phys. Chem. C* **2019**, *123*, 9388–9393. [[CrossRef](#)]
108. Lai, X.; Zhang, G.; Zeng, L.; Xiao, X.; Peng, J.; Guo, P.; Zhang, W.; Lai, W. Synthesis of PDA-Mediated Magnetic Bimetallic Nanozyme and Its Application in Immunochromatographic Assay. *ACS Appl. Mater. Interfaces* **2020**, *13*, 1413–1423. [[CrossRef](#)]
109. Gökçal, B.; Kip, Ç.; Tuncel, A. One-pot, direct glucose detection in human whole blood without using a dilution factor by a magnetic nanozyme with dual enzymatic activity. *J. Alloys Compd.* **2020**, *843*, 156012. [[CrossRef](#)]
110. Xu, X.; Wu, S.; Guo, D.; Niu, X. Construction of a recyclable oxidase-mimicking Fe<sub>3</sub>O<sub>4</sub>@MnO<sub>x</sub>-based colorimetric sensor array for quantifying and identifying chlorophenols. *Anal. Chim. Acta* **2020**, *1107*, 203–212. [[CrossRef](#)]
111. Wen, S.H.; Zhong, X.L.; Wu, Y.D.; Liang, R.P.; Zhang, L.; Qiu, J.D. Colorimetric assay conversion to highly sensitive electrochemical assay for bimodal detection of arsenate based on cobalt oxyhydroxide nanozyme via arsenate absorption. *Anal. Chem.* **2019**, *91*, 6487–6497. [[CrossRef](#)] [[PubMed](#)]
112. Cheng, H.; Zhang, L.; He, J.; Guo, W.; Zhou, Z.; Zhang, X.; Nie, S.; Wei, H. Integrated Nanozymes with Nanoscale Proximity for in Vivo Neurochemical Monitoring in Living Brains. *Anal. Chem.* **2016**, *88*, 5489–5497. [[CrossRef](#)] [[PubMed](#)]
113. Zhao, Z.; Huang, Y.; Liu, W.; Ye, F.; Zhao, S. Immobilized Glucose Oxidase on Boronic Acid-Functionalized Hierarchically Porous MOF as an Integrated Nanozyme for One-Step Glucose Detection. *ACS Sustain. Chem. Eng.* **2020**, *8*, 4481–4488. [[CrossRef](#)]
114. Shen, H.; Zhou, Z.; He, W.; Chao, H.; Su, P.; Song, J.; Yang, Y. Oligonucleotide-Functionalized Enzymes Chemisorbing on Magnetic Layered Double Hydroxides: A Multimodal Catalytic Platform with Boosted Activity for Ultrasensitive Glucose Detection. *ACS Appl. Mater. Interfaces* **2021**, *13*, 14995–15007. [[CrossRef](#)]
115. Wu, J.; Li, S.; Wei, H. Multifunctional nanozymes: Enzyme-like catalytic activity combined with magnetism and surface plasmon resonance. *Nanoscale Horiz.* **2018**, *3*, 367–382. [[CrossRef](#)]
116. Wang, N.; Shi, J.; Liu, Y.; Sun, W.; Su, X. Constructing bifunctional metalorganic framework based nanozymes with fluorescence and oxidase activity for the dualchannel detection of butyrylcholinesterase. *Anal. Chim. Acta* **2022**, *1205*, 339717. [[CrossRef](#)]
117. Lin, T.; Qin, Y.; Huang, Y.; Yang, R.; Hou, L.; Ye, F.; Zhao, S. A label-free fluorescence assay for hydrogen peroxide and glucose based on the bifunctional MIL-53(Fe) nanozyme. *Chem. Commun.* **2018**, *54*, 1762–1765. [[CrossRef](#)]
118. Ye, K.; Wang, L.; Song, H.; Li, X.; Niu, X. Bifunctional MIL-53(Fe) with pyrophosphate-mediated peroxidase-like activity and oxidation-stimulated fluorescence switching for alkaline phosphatase detection. *J. Mater. Chem. B* **2019**, *7*, 4794–4800. [[CrossRef](#)]
119. Li, X.; Liu, P.; Niu, X.; Ye, K.; Ni, L.; Du, D.; Pan, J.; Lin, Y. Tri-functional Fe–Zr bi-metal–organic frameworks enable high-performance phosphate ion ratiometric fluorescent detection. *Nanoscale* **2020**, *12*, 19383–19389. [[CrossRef](#)]
120. Guo, J.; Liu, Y.; Mu, Z.; Wu, S.; Wang, J.; Yang, Y.; Zhao, M.; Wang, Y. Label-free fluorescence detection of hydrogen peroxide and glucose based on the Ni-MOF nanozyme-induced self-ligand emission. *Mikrochim. Acta* **2022**, *189*, 219. [[CrossRef](#)]
121. Sun, Y.; Lin, T.; Zeng, C.; Jiang, G.; Zhang, X.; Ye, F.; Zhao, S. A self-correcting fluorescent assay of tyrosinase based on Fe-MIL-88B-NH<sub>2</sub> nanozyme. *Mikrochim. Acta* **2021**, *188*, 158. [[CrossRef](#)]
122. Liu, P.; Li, X.; Xu, X.; Ye, K.; Wang, L.; Zhu, H.; Wang, M.; Niu, X. Integrating peroxidase-mimicking activity with photoluminescence into one framework structure for high-performance ratiometric fluorescent pesticide sensing. *Sens. Actuators B Chem.* **2021**, *328*, 129024. [[CrossRef](#)]

123. Xu, X.; Luo, Z.; Ye, K.; Zou, X.; Niu, X.; Pan, J. One-pot construction of acid phosphatase and hemin loaded multifunctional metal–organic framework nanosheets for ratiometric fluorescent arsenate sensing. *J. Hazard. Mater.* **2020**, *412*, 124407. [[CrossRef](#)]
124. Guo, J.; Wu, S.; Wang, Y.; Zhao, M. A label-free fluorescence biosensor based on a bifunctional MIL-101(Fe) nanozyme for sensitive detection of choline and acetylcholine at nanomolar level. *Sens. Actuators B Chem.* **2020**, *312*, 128021. [[CrossRef](#)]
125. Hou, L.; Qin, Y.; Lin, T.; Sun, Y.; Ye, F.; Zhao, S. Michael reaction-assisted fluorescent sensor for selective and one step determination of catechol via bifunctional Fe-MIL-88NH<sub>2</sub> nanozyme. *Sens. Actuators B Chem.* **2020**, *321*, 128547. [[CrossRef](#)]
126. Li, S.; Hu, X.; Chen, Q.; Zhang, X.; Chai, H.; Huang, Y. Introducing bifunctional metal-organic frameworks to the construction of a novel ratiometric fluorescence sensor for screening acid phosphatase activity. *Biosens. Bioelectron.* **2019**, *137*, 133–139. [[CrossRef](#)]
127. Xia, Y.; Sun, K.; Zuo, Y.-N.; Zhu, S.; Zhao, X.-E. Fluorescent MOF-based nanozymes for discrimination of phenylenediamine isomers and ratiometric sensing of o-phenylenediamine. *Chin. Chem. Lett.* **2021**, *33*, 2081–2085. [[CrossRef](#)]
128. Liu, P.; Zhao, M.; Zhu, H.; Zhang, M.; Li, X.; Wang, M.; Liu, B.; Pan, J.; Niu, X. Dual-mode fluorescence and colorimetric detection of pesticides realized by integrating stimulus-responsive luminescence with oxidase-mimetic activity into cerium-based coordination polymer nanoparticles. *J. Hazard. Mater.* **2022**, *423*, 127077. [[CrossRef](#)]
129. Liu, P.; Zhu, H.; Wang, M.; Wei, M.; Liu, B.; Hu, P.; Lin, J.; Niu, X. Bimodal ratiometric fluorescence and colorimetric sensing of paraoxon based on trifunctional Ce,Tb co-coordinated polymers. *Sens. Actuators B Chem.* **2022**, *360*, 131616. [[CrossRef](#)]
130. Wu, Y.; Gao, Y.; Du, J. Bifunctional gold nanoclusters enable ratiometric fluorescence nanosensing of hydrogen peroxide and glucose. *Talanta* **2019**, *197*, 599–604. [[CrossRef](#)]
131. Wan, Y.; Zhao, J.; Deng, X.; Chen, J.; Xi, F.; Wang, X. Colorimetric and Fluorescent Dual-Modality Sensing Platform Based on Fluorescent Nanozyme. *Front. Chem.* **2021**, *9*, 774486. [[CrossRef](#)]
132. Li, X.; Ding, S.; Lyu, Z.; Tieu, P.; Wang, M.; Feng, Z.; Pan, X.; Zhou, Y.; Niu, X.; Du, D.; et al. Single-Atomic Iron Doped Carbon Dots with Both Photoluminescence and Oxidase-Like Activity. *Small* **2022**, *18*, 2203001. [[CrossRef](#)]
133. Zhang, W.; Li, X.; Xu, X.; He, Y.; Qiu, F.; Pan, J.; Niu, X. Pd nanoparticle-decorated graphitic C<sub>3</sub>N<sub>4</sub> nanosheets with bifunctional peroxidase mimicking and ON–OFF fluorescence enable naked-eye and fluorescent dual-readout sensing of glucose. *J. Mater. Chem. B* **2018**, *7*, 233–239. [[CrossRef](#)]
134. Gooding, J.J. Can Nanozymes Have an Impact on Sensing? *ACS Sens.* **2019**, *4*, 2213–2214. [[CrossRef](#)]
135. Zhou, Y.; Liu, B.; Yang, R.; Liu, J. Filling in the Gaps between Nanozymes and Enzymes: Challenges and Opportunities. *Bioconjugate Chem.* **2017**, *28*, 2903–2909. [[CrossRef](#)]
136. Ruan, X.; Hulubei, V.; Wang, Y.; Shi, Q.; Cheng, N.; Wang, L.; Lyu, Z.; Davis, W.C.; Smith, J.N.; Lin, Y.; et al. Au@PtPd enhanced immunoassay with 3D printed smartphone device for quantification of diaminochlorotriazine (DACT), the major atrazine biomarker. *Biosens. Bioelectron.* **2022**, *208*, 114190. [[CrossRef](#)] [[PubMed](#)]